Full Paper

Applied Organometallic Chemistry

Received: 27 June 2008 Revised: 17 July 2008 Accepted: 18 July 2008 Published online in Wiley Interscience: 1 September 2008

(www.interscience.com) DOI 10.1002/aoc.1451

# Syntheses, characterization and anti-microbial activities of palladium(II) and palladium(IV) complexes of 3,10-C-*meso*-$Me_8$[14]diene ($L^1$) and its reduced isomeric *anes* ($L_A$, $L_B$ and $L_C$). Crystal and molecular structure of $[PdL^1][Pd(SCN)_4]$

**Tapashi G. Roy[a], Saroj K. S. Hazari[a], Kanak K. Barua[a], Dong Il Kim[b], Yu Chul Park[b] and Edward R.T. Tiekink[c]***

**The reactions of 3,10-C-*meso*-3,5,7,7,10,12,14,14-octamethyl-1,4,8,11-tetraazacyclotetradecadiene, $L^1$, and two isomers ($L_B$ and $L_C$, differing in the orientation of methyl groups on the chiral carbon atoms) of its reduced form with $PdCl_2$ and $K_2[Pd(SCN)_4]$, produce square-planar tetrachloro- and tetrathiocyano-palladium(II) complexes of general formulae $[PdL'][PdCl_4]$ and $[PdL'][Pd(SCN)_4]$ ($L' = L^1$, $L_B$ and $L_C$), respectively. By contrast, the third *ane* isomer, $L_A$, upon reaction with the same reagents, $PdCl_2$ and $K_2[Pd(SCN)_4]$, formed octahedral tetrachloro- and tetrathiocyanato-palladium(IV) complexes $[PdL_ACl_2]Cl_2$ and $[PdL_A(SCN)_2](SCN)_2$, respectively. The $[PdL'][PdCl_4]$ and $[PdL_ACl_2]Cl_2$ complexes undergo substitution reactions with KSCN to form square-planar and octahedral tetrathiocyanato complexes $[PdL'][Pd(SCN)_4]$ and $[PdL_A(SCN)_2](SCN)_2$, respectively. All complexes have been characterized on the basis of analytical, spectroscopic, conductometric and magnetochemical data. The anti-fungal and anti-bacterial activities of these complexes have been studied against some phytopathogenic fungi and bacteria. The crystal structure of $[PdL^1][Pd(SCN)_4]$ has been confirmed by X-ray crystallography and shows with square-planar $PdN_4$ and $PdS_4$ geometries [monoclinic, space group $C2/c$, $a = 17.884(3)$ Å, $b = 14.734(2)$ Å, $c = 11.4313(18)$ Å, $\beta = 104.054(5)°$].** 

*Supporting information may be found in the online version of this article.*

**Keywords:** palladium(II); palladium(IV); tetraazacyclotetradecadiene; tetraazacyclodecanes; anti-fungal activity; anti-bacterial activity; crystal structure

## Introduction

The importance of the tetraaza-macrocyclic ligands and their complexes is now well recognized due to their high thermodynamic stability, kinetic inertness and their structural similarity to natural macrocyclic complexes such as vitamin $B_{12}$, haemoglobin, chlorophyll, etc. which play multiple roles in biological systems.[1,2] In the realm of biological applications, metal complexes of compounds related to cyclam (14-membered tetraaza macrocyclic ligands) have been explored for their use in magnetic resonance imaging (MRI) and radioimmunotherapy.[3,4] They are also important for their applications in pharmacological,[5] industrial,[6] crystal engineering[7] and analytical[8] fields. Their importance also relates to their anti-fungal[9] and anti-bacterial[10,11] activities. In addition, research on macrocyclic complexes has demonstrated potential anti-cancer activity.[12,13]

Against this background, the copper, nickel, cobalt, zinc and cadmium complexes of 3,10-C-*meso*-$Me_8$[14]diene ($L^1$), its reduced isomeric anes ($L_A$, $L_B$ and $L_C$) (Fig. 1) and their N-substituted ligands have been synthesized and explored for their anti-fungal and anti-bacterial activities, often showing moderate activity.[14–18] It is the latter application that motivates much of our interest in this area and which has also led to a number of structural studies.[10,11,19–22]

As a continuation of our interest in the chemistry of such metal complexes and their potential applications as anti-fungal and bacterial agents, it was thought of interest to extend the chemistry to investigate palladium complexes. Herein, the syntheses, characterization and anti-microbial studies of square-planar mixed palladium(II) complexes of general formula $[PdL'][PdX_4]$ (where $L' = L^1$, $L_B$ or $L_C$; and X = Cl or NCS) and octahedral palladium(IV)

* *Correspondence to: Edward R.T. Tiekink, Department of Chemistry, University of Texas at San Antonio, TX 78249-0698, USA. E-mail: Edward.Tiekink@utsa.edu*

a *Department of Chemistry, University of Chittagong, Chittagong 4331, Bangladesh*

b *Department of Chemistry, Kyungpook National University, Daegu 702-701, Korea*

c *Department of Chemistry, University of Texas at San Antonio, TX 78249-0698, USA*

 

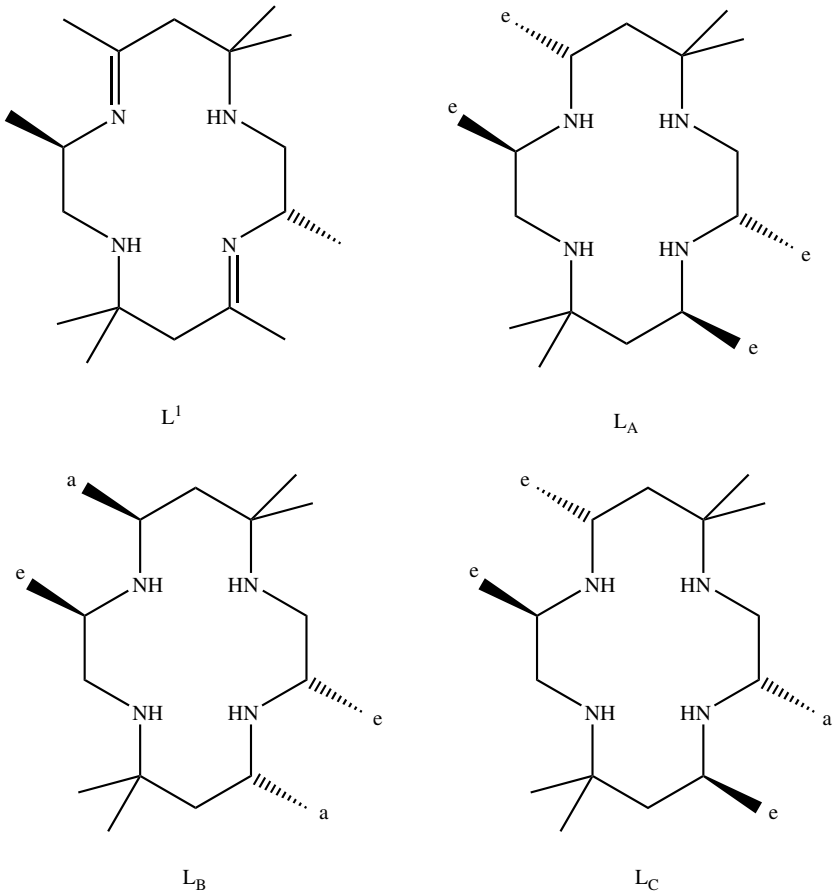


**Figure 1.** Chemical structures of macrocyclic ligands, $L^1$, $L_A$, $L_B$ and $L_C$.

complexes of $L_A$, $[PdL_AX_2]X_2$, are described. As well, the crystal and molecular structure of a representative derivative, namely $[PdL^1][Pd(SCN)_4]$, is reported.

## Experimental

### General comments

1,2-Diaminopropane, $HClO_4$, sodium borohydride (Merck Germany), $PdCl_2.xH_2O$ (Aldrich, USA), KSCN, $KNO_3$ and $KNO_2$ (Fluka AG, Switzerland) were used as received from commercial sources. The solvents used in the reactions were of AR-grade and were obtained from commercial sources (Merck, Germany). The solvents were dried using standard literature procedures.

### Measurements

Microanalyses (C, H, N and S) were performed on a Carlo-Ebra, EA 1108 instrument. Palladium and chloride were analysed at Kyungpook National University, South Korea. Infrared spectra were measured in the range 400–4000 $cm^{-1}$ on a Matterson Instruments Inc. Glaxy 7020 A spectrophotometer as KBr pellets. Electronic absorption spectra were recorded on a Shimadzu UV–visible 265 spectrophotometer. The mass spectral measurements of the ligands were carried out on a Varian MAT 311A (70 eV, EI) instrument and those of complexes were carried on a Jeol MS-DX300 gas chromatograph mass spectrometer at 70 eV using a direct inlet system. $^1H$ and $^{13}C$ NMR spectra were recorded on a 300 MHz Bruker NMR spectrometer at room temperature and chemical shifts in DMSO-$d_6$ are given in p.p.m. relative to tetramethylsilane as an internal reference. Conductance measurements were performed in DMSO solutions, using a HANNA instrument equipped with a HI 8820N conductivity cell. Magnetic measurements were carried out with a Gouy balance, calibrated against $Hg[Co(NCS)_4]$; susceptibilities were corrected for diamagnetic increments.

### Syntheses

*Preparation of macrocycles*

Synthesis of the parent ligand, 3,10-C-*meso*-$Me_8$[14]diene dihydroperchlorate, $L^1{\cdot}2HClO_4$,[23] isolation of free diene,[15] $L^1$, and reduction of this diene and separation of the isomeric $Me_8$[14]anes to produce $L_A$, $L_B$ and $L_C$ were performed according to literature methods.[24,25]

### Synthesis of the tetrachloropalladium(II) complex of $L^1$, $[PdL^1][PdCl_4]$ (1)

$L^1$ (0.308 g, 1.0 mmol) and palladium(II) chloride (0.354 g, 2.0 mmol)) were dissolved separately in hot methylcyanide (150 ml). The ligand solution was added dropwise to metal solution while hot. The mixture was heated under reflux for 24 h. A yellow-orange product started to appear after 30 min heating. The products were filtered hot and washed with methylcyanide several times, followed by ethanol and diethyl ether. Then the

products were dried under vacuum for 24 h, and finally stored in a desiccator over silica gel. Analytically pure products were obtained after recrystallization from a DMSO solution of the complex.

The tetrachloropalladium(IV) complex of $L_A$, $[PdL_ACl_2]Cl_2$ (**2**), and the tetrachloropalladium(II) complexes of $L_B$ and $L_C$, $[PdL_B][PdCl_4]$ (**3**) and $[PdL_C][PdCl_4]$ (**4**) were prepared analogously, using palladium(II) chloride and appropriate ligands.

### Synthesis of tetrathiocyanatopalladium(II) complex of $L^1$, $[PdL^1][Pd(SCN)_4]$ (5)

This complex was prepared using two methods.

*Method 1*

$[PdL^1][PdCl_4]$ (0.662 g, 1.0 mmol) was suspended in methanol (200 ml) and KSCN (0.582 g, 6.0 mmol) was added. The suspension was heated under reflux for 24 h. The yellow products started to change to brick-red after heating for about 40 min. The brick-red products were filtered hot, washed several times with hot methanol, followed by ethanol and diethyl ether and finally dried in a desiccator over silica gel.

*Method 2*

$PdCl_2$ (0.177 g, 1.0 mmol) was dissolved in methanol (100 ml) containing KSCN (0.582 g, 6.0 mmol) by heating for 45 min. The resulting blood-red solution was allowed to stand for 1 h at room temperature. The mixture was then filtered and the blood-red filtrate was again heated for 15 min. To this, a hot methanol solution (100 ml) of $L^1$ (0.308 g, 1.0 mmol) was added slowly. The brick-red precipitate appeared within a few minutes. The resulting mixture was refluxed for 24 h. The solid product was filtered hot, washed with methanol, followed by ethanol and diethyl ether, and finally dried in a desiccator over silica gel. The product was found to give the same analytical and spectral analyses as observed for the product prepared by method 1.

The tetrathiocyanatopalladium(IV) complex of $L_A$, $[PdL_A(SCN)_4]$ (**6**), and the tetrathiocyanatopalladium(II) complexes of $L_B$ and $L_C$, $[PdL_B][Pd(SCN)_4]$ (**7**) and $[PdL_C][Pd(SCN)_4]$ (**8**), were also synthesized following both methods outlined above.

### Anti-microbial studies

*Determination of anti-fungal activities*

The *in vitro* anti-fungal activities of the complexes against selected phytopathogenic fungi were assessed by the poisoned food technique. Potato dextrose agar (PDA) was used as a growth medium. DMSO was used as the solvent to prepare solutions of compounds. The solutions were then mixed with the sterilized PDA so as to maintain concentrations of the compounds of 0.01%. Aliquots of 20 ml of these solutions were each poured into a Petri dish. After the medium had solidified, a 5 mm mycelial disc of each fungus was placed in the centre of each assay plate, along with a control. Linear growth of the fungus was measured in millimetres after 5 days of incubation at $25 \pm 2\,^{\circ}C$.

*Determination of anti-bacterial activities*

The anti-bacterial activities of the test materials were measured by the disc diffusion method. Paper discs of 6 mm diameter and Petri plates of 70 mm diameter were used throughout. Pour plates were prepared from sterilized molten Nutrient Agar (NA) at 45 °C. After solidification of the pour plates, suspensions of the test organisms were spread uniformly over the pour plate with a sterilized glass rod. After soaking the paper discs with the test chemicals (1% in DMSO solutions), they were placed in the centre of the inoculated pour plate. A control plate was maintained in each case with DMSO only. The plates were kept for 4 h at low temperature (4 °C) in order to allow the test chemicals to diffuse from the paper disc to the surrounding medium. The plates were then incubated at $37 \pm 2\,^{\circ}C$ for growth of the test organisms, and checked at 24 and 48 h intervals. The anti-bacterial activity was expressed in terms of the diameter (in mm) of the zone of inhibition.

### Crystal structure determination

The crystals of $[PdL^1][Pd(SCN)_4]$ suitable for the X-ray diffraction study were prepared by slow crystallization of a DMSO–acetonitrile (3 : 1) solution of the compound. Intensity data were collected at 153 K on a Rigaku AFC12/Saturn724 CCD fitted with Mo K$\alpha$ radiation. The data set was corrected for absorption effects based on multiple scans[26] and reduced using standard methods.[27] The structure was solved by direct-methods[28] and refined by a full-matrix least-squares procedure on $F^2$ with anisotropic displacement parameters for non-hydrogen atoms, hydrogen atoms in their calculated positions and a weighting scheme of the form $w = 1/[\sigma^2(F_o^2) + (0.027P)^2 + 3.505P]$ where $P = (F_o^2 + 2F_c^2)/3)$.[29] Crystal data and refinement details are given in Table 1. Figure 2, showing the atom labelling scheme, was drawn with 50% displacement ellipsoids using ORTEP[30] and the remaining figures were drawn with DIAMOND.[31]

**Table 1.** Crystal data and refinement details for $[PdL^1][Pd(SCN)_4]$ (**5**)

| | |
|---|---|
| Formula | $C_{22}H_{36}N_8Pd_2S_4$ |
| Formula weight | 753.63 |
| Crystal habit, colour | Block, orange |
| Crystal system | Monoclinic |
| Space group | $C2/c$ |
| $a$ (Å) | 17.884(3) |
| $b$ (Å) | 14.734(2) |
| $c$ (Å) | 11.4313(18) |
| $\beta$ (deg) | 104.054(5) |
| Volume (Å$^3$) | 2921.9(8) |
| $Z$ | 4 |
| Density (calculated) | 1.713 |
| Absorption coefficient (mm$^{-1}$) | 1.544 |
| $F$(000) | 1520 |
| Crystal size (mm) | 0.10 × 0.20 × 0.25 |
| $\theta$ range for data collection (deg) | 2.4–26.5 |
| Reflections collected | 15 403 |
| Independent reflections | 3029 |
| $R_{int}$ | 0.018 |
| Reflections with $I \geq 2\sigma(I)$ | 2934 |
| Number of parameters | 167 |
| Goodness-of-fit on $F^2$ | 1.12 |
| Final $R$ indices [$I \geq 2\sigma(I)$] | $R_1 = 0.021$, $wR_2 = 0.022$ |
| $a$, $b$ for weighting scheme | 0.027, 3.505 |
| $R$ indices [all data] | $R_1 = 0.056$, $wR_2 = 0.057$ |
| Largest difference peak and hole (e Å$^{-3}$) | 0.39, −0.50 |
| CCDC deposition no. | 691 853 |

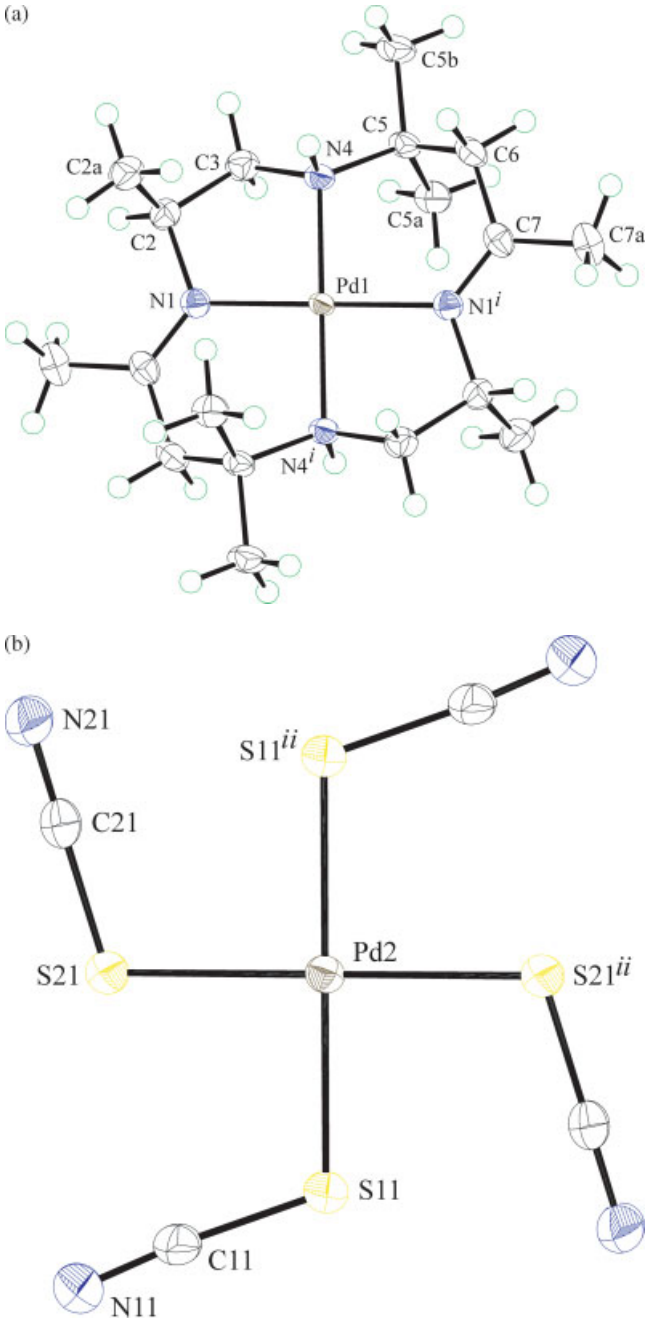


**Figure 2.** 2Molecular structures of (a) [PdL$^1$] and (b) [Pd(SCN)$_4$] in **5** showing the atom labelling schemes. Displacement ellipsoids are drawn at 50% probability level. Symmetry operations *i*: $1\frac{1}{2} - x, \frac{1}{2} - y, 1 - z$; and *ii*: $\frac{1}{2} - x, \frac{1}{2} - y, 1 - z$.

Data manipulation and interpretation were accomplished using teXsan[32] and PLATON.[33]

## Results and Discussion

### Synthesis

On the basis of MS,[15,24] $^1$H- and $^{13}$C{$^1$H}- NMR spectra[15,23,25] and X-ray crystallography,[25] the structures of $L^1$, $L_A$ $L_B$ and $L_C$ were established as indicated in Fig. 1. $L^1$, $L_B$, $L_C$ interact with $PdCl_2$ and $K_2Pd(SCN)_4$ to produce square-planar palladium(II) complexes of general formula [PdL′][PdCl$_4$] (where L′ = $L^1$, $L_B$, or $L_C$) (**1, 3, 4**) and [PdL′][Pd(SCN)$_4$] (**5, 7, 8**), respectively, whereas $L_A$ reacts distinctly with the same reagents to produce the octahedral palladium(IV) complexes [PdL$_A$Cl$_2$]Cl$_2$ (**2**) and [PdL$_A$(SCN)$_2$](SCN)$_2$ (**6**), respectively. Moreover **1**–**4** were found to undergo ligand substitution reactions with KSCN to produce the thiocyanato complexes, **5**–**8**, respectively. All of the complexes were characterized by IR, UV–vis and NMR spectroscopy, as well as by analytical, magnetochemical and conductance measurements and, in the case of **5**, by single crystal X-ray diffraction analysis. Physical and analytical data are summarized in Table 2.

All the complexes are found to be diamagnetic as expected for the square-planar palladium(II) complexes, **1, 3**–**5, 7** and **8** ($dsp^2$ hybridisation). However, for the octahedral palladium(IV) complexes, **2** and **6**, two possibilities exist. Thus, for $d^2sp^3$ (inner) hybridization, diamagnetism is expected but for $sp^3d^2$ (outer) hybridization, paramagnetism corresponding to four unpaired electrons is expected. Since these complexes are diamagnetic, $d^2sp^3$ (inner) hybridization is in effect.

### Chloro complexes (1–4)

The interaction of $PdCl_2 \cdot xH_2O$ with $L^1$ and $L_A$ in acetonitrile solution yielded yellow-orange products and the same reaction with $L_B$ and $L_C$ produced yellow products. It is surprising to note that the diene ligand in its dihydroperchlorate form did not react at all, although the free ligand underwent reaction with $PdCl_2$ easily. Moreover, it was also observed that these ligands did not undergo complexation with $PdCl_2$ in solvents such as methanol, ethanol, DMF or DMSO, but rather gave intractable black products.

In the preparation of these chloro complexes, if the ligand ratios of $L^1$, $L_B$ or $L_C$ were higher than the required amount, some white products were obtained with higher percentage of C, H, N, but the analyses did not match with any anticipated formulae. However, $L_A$ reacts with palladium chloride in any ratio to produce a complex of the same formula, i.e. [PdL$_A$Cl$_2$]Cl$_2$.

The molar conductivity values (Table 2) of 62–64 ohm$^{-1}$ cm$^2$ mol$^{-1}$ in DMSO of **1, 3** and **4** indicate that the complexes are 1:1 electrolytes, as expected for the assigned formulae. However, the conductivity value of 52 ohm$^{-1}$ cm$^2$ mol$^{-1}$ determined for **2** deviates significantly from the expected value for a 1:2 electrolyte, which may be due to an equilibrium between two structures as shown in equation (1):

$$[PdL_ACl_2]Cl_2 \rightleftharpoons [PdL_ACl_4] \quad (1)$$

While not implying a coordination number greater than 6 for the palladium(IV) centre, some association between all chloride anions and the complex is implied in DMSO solution, thereby reducing the conductivity of the solution.

The infrared spectra of these complexes displayed the expected νN–H bands at 3089–3275, νC–C at 1135–1195, νC–H at 2966–2979, νPd–N at 518–588 and $\nu CH_3$ at 1373–1398 cm$^{-1}$; see Table 3 for data. The mass spectra of the complexes **1**–**3** revealed *m/z* values 663, 561 and 667, respectively, corresponding to their molecular ion peaks; complex **4**, [PdL$_C$][PdCl$_4$], did not ionize at all.

The electronic spectra of all complexes exhibit two bands in the UV region in the range 256–305 nm, Table 4. These bands are attributable to charge transfer bands from metal to ligand.[34] These complexes further show two additional bands and shoulders in the range 332–407 nm. However, complex **2** shows only one

**Table 2.** Physical and analytical data for **1**–**8**

| Complex | Molecular formula | Elemental composition: found (calcd) (%) C | H | N | Cl | S | Pd | Colour | Melting point (°C) | Conductance in DMSO (ohm$^{-1}$ cm$^2$ mol$^{-1}$) |
|---|---|---|---|---|---|---|---|---|---|---|
| **1** | $C_{18}H_{36}N_4Cl_4Pd_2$ | 32.15 (32.60) | 5.43 (5.47) | 8.60 (8.45) | 21.38 (21.38) | – | 32.02 (32.09) | Yellow | 310 (dec.) | 64 |
| **2** | $C_{18}H_{40}N_4Cl_4Pd$ | 38.69 (38.55) | 7.49 (7.19) | 10.05 (9.99) | 25.20 (25.29) | – | 18.86 (18.98) | Yellow-orange | 320 (dec.) | 42 |
| **3** | $C_{18}H_{40}N_4Cl_4Pd_2$ | 32.75 (32.40) | 6.34 (6.04) | 8.30 (8.40) | 20.98 (21.25) | – | 31.79 (31.90) | Light-yellow | 344 (dec.) | 64 |
| **4** | $C_{18}H_{40}N_4Cl_4Pd_2$ | 33.00 (32.40) | 6.71 (6.04) | 8.37 (8.40) | 21.11 (21.25) | – | 32.05 (31.90) | Light-yellow | 334 (dec.) | 62 |
| **5** | $C_{22}H_{36}N_8S_4Pd_2$ | 35.22 (35.06) | 4.87 (4.81) | 15.10 (14.87) | – | 16.56 (17.02) | 28.17 (28.24) | Brick-red | 280 (dec.) | 60 |
| **6** | $C_{22}H_{40}N_8S_4Pd$ | 40.62 (40.57) | 6.55 (6.19) | 17.09 (17.21) | – | 19.24 (19.69) | 16.25 (16.34) | Brick-red | 260 | 64 |
| **7** | $C_{22}H_{40}N_8S_4Pd_2$ | 34.98 (34.87) | 5.34 (5.32) | 14.75 | – (14.79) | 16.79 (16.93) | 28.22 (28.09) | Brick-red | 300 (dec.) | 54 |
| **8** | $C_{22}H_{40}N_8S_4Pd_2$ | 34.94 (34.87) | 5.39 (5.32) | 14.74 (14.79) | – | 16.89 (16.93) | 28.06 (28.09) | Brick-red | 280 (dec.) | 60 |

**Table 3.** IR spectral data (cm$^{-1}$) for **1**–**8**[a]

| | υ N–H | υ C–H | $\upsilon CH_3$ | υ C–C | υ C=N | υ Pd–N | υ CN | υ CS | υ NCS |
|---|---|---|---|---|---|---|---|---|---|
| **1** | 3275 (vs) | 2969 (vs) | 1396 (s) | 1135 (s) | 1653 (vs) | 540 (w) | | | |
| **2** | 3217 (vs) | 2966 (vs) | 1383 (s) | 1162 (s) | | 572 (m) | | | |
| **3** | 3139 (s) | 2979 (s) | 1380 (s) | 1161 (s) | | 581 (m) | | | |
| **4** | 3126 (s) | 2971 (s) | 1373 (s) | 1178 (s) | | 518 (w) | | | |
| **5** | 3145 (s) | 2968 (m) | 1374 (m) | 1164 (m) | 1653 (s) | 588 (vw) | 2108 (vs) | 700 (w) | 420 (w) |
| **6** | 3245 (s) | 2975 (s) | 1381 (s) | 1163 (m) | | 573 (m) | 2109 (vs) | 695 (w) | 415 (w) 420 (w) |
| **7** | 3170 (s) 3200 (s) | 2971 (s) | 1398 (s) | 1195 (s) | | 584 (m) | 2117 (vs) | 700 (m) | 425 (m) |
| **8** | 3124 (s) | 2973 (s) | 1374 (s) | 1174 (s) | | – | 2111 (vs) | 700 (vw) | 420 (m) |

[a] vs, very strong; s, strong; m, medium; w, weak; vw, very weak.

**Table 4.** Electronic and mass spectral data for **1**–**8**

| | $\lambda_{max}$ in nm ($\varepsilon_{max}$) in DMSO[a] | | | | Molecular ion peak at *m/z* |
|---|---|---|---|---|---|
| **1** | 399 (990) h | 337 (3300) sh | 305 (5600) | 256 (25000) | 663 |
| **2** | 407 (1600) h | | 303 (9100) | 258 (25700) | 561 |
| **3** | 407 (1000) h | 337 (4800) sh | 302 (9600) | 257 (25000) | 667 |
| **4** | 404 (1000) h | 332 (4200) sh | 300 (8000) | 257 (25000) | Not obs. |
| **5** | | | 315 (22000) | 254 (45000) | Not obs. |
| **6** | | | 315 (23500) | 254 (44700) | 652 |
| **7** | | | 315 (23600) | 254 (45300) | Not obs. |
| **8** | | | 315 (22700) | 254 (45000) | Not obs. |

[a] $\lambda_{max}$ (nm) = Wavelength of absorbance maxima in nm; $\varepsilon$ = molar extinction coefficient in dm$^3$ mol$^{-1}$ cm$^{-1}$; h = hump, sh = shoulder.

band at 407 nm. These weaker bands are attributed to charge transfer transitions from the highest occupied ligand molecular orbital to lowest empty *d* orbital of palladium.[35] Since the molar extinction coefficients of these complexes are much higher than those normally assigned to ligand field transitions, the ligand field bands are not assigned to these complexes as these are obscured by charge transfer bands of high intensity.

### NMR spectra

The assignments for the $^1$H NMR spectra are given in Table 5 and those for the $^{13}$C NMR in Table 6. Assignments are made on the basis of literature studies[17,18,36–40] and are consistent with the expected formulae. The upfield singlets in the region 1.21–1.39 ppm and downfield singlets at 1.35–1.49 ppm have been assigned to equatorial and axial gem-dimethyl protons, respectively. The appearance of a downfield singlet at 2.29 ppm in complex **1** has been assigned to methyl groups bound to the $sp^2$ carbon atoms. Similarly, upfield doublets (equatorial) and

**Table 5.** $^{1}$H NMR chemical shifts and coupling data (ppm and Hz) for **1**–**8**[a]

| | Types of protons | | | |
|---|---|---|---|---|
| | Geminal dimethyl $\delta$ (ppm) | Methyl on chiral carbon $\delta$ (ppm) | Methyl on $sp^2$ carbon $\delta$ (ppm)[b] | $CH_2$, CH and NH $\delta$ (ppm) |
| **1** | 1.28 (os, 6H, e) | 1.03–1.05 (d, 3H, e)[5]c | 2.29 (s, 6H) | 2.67(m), 3.00 (m), 4.36 (m), 4.67 (m), 4.77 (m), 4.85 (m) |
| | 1.40 (s, 6H, a) | 1.27–1.29 (od, 3H, e)[5]c | | |
| **2** | 1.21 (s, 6H, e) | 1.02–1.03 (d, 6H, e)[4]c | | 1.40 (m), 1.74 (m), 2.80 (m), 3.21 (m) |
| | 1.35 (s, 6H, a) | 1.09–1.11 (d, 6H, a)[4]c | | |
| **3** | 1.27 (s, 6H, e) | 1.16–1.17 (d, 6H, e)[5]c | | 1.68–1.70 (d, 4H)[6]c, 1.87 (m), 2.15 (m), 2.75 (m), 2.94 (m), 3.17 (m) |
| | 1.49 (s, 6H, a) | 1.31–1.33 (d, 6H, a)[5]c | | |
| **4** | 1.39 (s, 6H, e) | 1.08–1.10 (d, 3H, e)[6]c | | 1.64 (m), 2.92 (m), 1.81 (m), 2.63 (m) |
| | 1.44 (s, 3H, a) | 1.11–1.13 (d, 6H, e)[6]c | | 2.86 (m), 2.95 (m) |
| | | 1.18–1.20 (d, 3H, a)[6]c | | |
| **5** | 1.26 (os, 6H, e) | 1.26–1.28 (od, 6H, e)[6]c | 2.29 (s, 6H) | 2.69 (m), 2.96 (m), 3.10 (m), 3.25 (m) |
| | 1.40 (s, 6H,a) | | | |
| **6** | 1.22 (s, 6H, e) | 1.01–1.02 (d, 6H, e)[5]c | | 1.46 (m), 1.68 (m), 2.83 (m), 3.01 (m) |
| | 1.33 (s, 6H, a) | 1.08–1.09 (d, 6H, a)[5]c | | |
| **7** | 1.20 (s, 6H,e) | 1.09–1.10 (d, 6H, e)[5]c | | 1.69 (d, 4H)[5]c |
| | 1.43 (s, 6H, a) | 1.23–1.25 (d, 6H, e)[5]c | | 2.56 (m), 2.63 (m), 2.87 (m), 3.01 (m) |
| **8** | 1.42 (s, 6H, e) | 1.12–1.14 (d, 3H, e)[6]c | | 2.47 (m), 2.68 (m) |
| | 1.47 (s, 6H, a) | 1.15–1.17 (d, 6H, e)[6]c | | 2.87 (m), 3.11 (m) |
| | | 1.22–1.24 (d, 3H, a)[6]c | | |

[a] Multiplicity is given as s, singlet; d, doublet; m, multiplet; os, overlapped singlets; od, overlapped doublets. [b] a = axial; e = equatorial. [c] $J$(H–H) in Hz.

**Table 6.** $^{13}$C{$^{1}$H}-NMR spectral data for **1**–**8**

| | | Types of carbons $\delta$ (ppm) | | | |
|---|---|---|---|---|---|
| | No of signals | Peripheral | Ring | Double bonded ring | NCS |
| $L^1$ | 18 (8 + 8 + 2) | 19.5, 19.9, 22.9, 24.5, 28.2, 28.8, 32.0, 32.8 | 46.6, 48.1, 48.9, 49.6, 50.4, 52.5, 55.5, 59.1 | 167.7 | |
| | | | | 171.9 | |
| **1** | 9 (4 + 4 + 1) | 16.7, 18.3, 22.8, 24.2 | 52.3, 55.4 56.6, 61.7 | 158.4 | |
| **5** | 10 (4 + 4 + 1 + 1) | 16.8, 21.1 21.4, 22.8 | 50.6, 52.4, 55.2, 60.3 | 178.8 | 185.0 |
| $L_A$ | 9 (4 + 5) | 4 signals (15–30) | 5 signals (40–60) | | |
| **2** | 9 (4 + 5) | 15.4, 18.9, 24.6, 25.3 | 41.6, 45.4, 48.3, 56.5, 58.5 | | |
| **6** | 10 (4 + 5 + 1) | 15.4, 19.0, 24.6, 25.2 | 40.8, 45.4, 46.0, 46.2, 58.7 | | 182.4 |
| $L_B$ | 9 (4 + 5) | 4 signals (15–30) | 5 signals (40–65) | | |
| **3** | 9 (4 + 5) | 15.1, 16.8, 23.2. 24.7, | 46.8, 48.9, 51.0, 52.8, 55.3 | | |
| **7** | 10 (4 + 5 + 1) | 15.6, 17.4 23.8, 25.2 | 47.4, 48.9, 51.5, 53.5, 55.9 | | 178.5 |
| $L_C$ | 18 (8 + 10) | 8 signals (15–30) | 10 signals (40–60) | | |
| **4** | 18 (8 + 10) | 16.5, 17.4, 18.4, 22.7, 25.1, 25.2, 25.8, 27.6 | 48.6, 50.5, 52.4, 53.0, 54.7, 55.0, 55.4, 55.7, 59.8, 61.1 | | |
| **8** | 19(8 + 10 + 1) | 12.2, 16.6, 18.2, 22.7, 23.5, 25.1, 25.7, 27.6 | 48.1, 48.7, 48.9, 50.6, 52.7, 53.5, 54.8, 55.3, 55.8, 61.1 | | 119.3 |

downfield (axial) doublets have been assigned to methyl groups on chiral carbon atoms. In case of complex **1,** an overlapped pattern at 1.27–1.29 ppm has been resolved for a singlet and a doublet. An additional downfield doublet at 1.69 ppm, assigned to $\beta$-methylene protons, has been identified for **3**. Thus, an 'all equatorial' orientation of double-bonded methyls and chiral methyls in **1**, a 'diaxial–diequatorial' orientation of chiral methyls in **2** and **3**, and a 'triequatorial–axial' orientation in **4** have been assigned. The coupling constants for all doublets due to ($CH_3$-H) and ($CH_2$-H) are in the range of 4–6 Hz. Other downfield multiplets have been accounted for by $CH_2$, CH and NH protons. The number of $^{13}$C NMR signals observed correspond to number of non-equivalent carbon atoms.[40] It is noted that, while the ligand $L^1$ displays 18 signals for 18 carbon nuclei, in its complex **1** only nine signals are observed owing to pair-wise equivalency of carbons having a symmetric 'all equatorial' orientation. Similarly the appearance of nine (same as the number of signals as observed in the spectra of their symmetric ligands $L_A$ and $L_B$) signals in **2** and **3** is due to their symmetric 'diaxial–diequatorial' orientation. However, 18 signals (the same as the number of signals appearing in the spectrum of its ligand $L_C$) in **4** have been accounted for due to its non-symmetric 'triequatorial–axial' orientation.

From the above analysis it is noted that, although the reactions of $L^1$, $L_B$ and $L_C$ with palladium(II) chloride produced

dimetallic palladium(II) with square-planar geometries, $L_A$ yielded a complex six-coordinated octahedral palladium(IV) complexes under the same condition without the addition of oxidant. The same phenomenon was observed during the reactions between cobalt(II) bromide (T. G. Roy, unpublished results) with these isomeric ligands ($L_A$, $L_B$ and $L_C$) under nitrogen. In that case, under the same reaction conditions, $L_B$ and $L_C$ gave pink dibromo cobalt(II) complex, whereas cobalt(II) was oxidized to green cobalt(III) when reacted with $L_A$. This phenomenon of oxidation of cobalt(II) to cobalt(III) and palladium(II) to palladium(IV) by $L_A$ may be accounted for by its different stereochemistry. In one study, it was noted that even $H_2O$ oxidized palladium(II) to palladium(IV) and there $H_2O$ was reduced to hydrogen (A. Canty, private communication).

### Thiocyanato complexes (5–8)

The reaction of $K_2Pd(SCN)_4$ (produced by the *in situ* reaction of $PdCl_2$ with KSCN in methanol solution) with $L^1$, $L_A$, $L_B$ and $L_C$ yielded brick-red products of molecular formula $Pd_2L'(SCN)_4$ ($L' = L^1$, $L_B$ and $L_C$) for $L^1$, $L_B$ and $L_C$, and $PdL_A(SCN)_4$ for the reaction with $L_A$. The same products were also produced by the substitution reactions performed on $Pd_2L'Cl_4$ and $PdL_ACl_4$ with KSCN in methanol solution. Attempts to carry out substitution reactions with $NO_3^-$ and $NO_2^-$ were unsuccessful. Analytical results, Table 2, support the proposed formulations.

The trends in molar conductivity values, Table 2, followed those for the analogous chloro complexes. Infrared spectra of these complexes, Table 3, exhibit the anticipated $\nu$N–H bands at 3124–3245, $\nu$C–C at 1163–1195, $\nu$C–H at 2968–2975, $\nu$Pd–N at 573–588 and $\nu CH_3$ at 1374–1398 $cm^{-1}$. The presence of the $\nu$CN bands at 2104–2117, $\nu$CS at 695–700 and some low-intensity $\delta$NCS bands at 415–425 $cm^{-1}$ are consistent with the coordination of thiocyanate ions via the sulfur atom. The position of the $\nu$CN bands at around 2100 $cm^{-1}$ clearly indicates that these complexes are sulfur-bonded thiocyanato complexes.[43] This conclusion is confirmed by an X-ray structure determination of **5**, see below.

The mass spectra of all the complexes could not be taken as all but one of the complexes did not vaporize under the experimental conditions employed, Table 2. The electronic spectra of the thiocyanato complexes exhibit two bands at 254 and 315 nm in the UV region. These bands may be attributed to charge transfer bands from metal to ligand,[35] as observed in corresponding chloro complexes. Compared with the chloro analogues, the bands at 254 nm are shifted to shorter wavelength by only 3–4 nm and those at 315 nm are shifted by about 15 nm to longer wavelength, see Table 4. The molar absorption coefficients of these complexes are greater than for the corresponding chloro complexes. Unlike, the thiocyanato complexes, they do not display any features around 400 and 335 nm. Since the molar extinction coefficients of these complexes are much higher than those normally assigned to ligand field transitions, the ligand field bands are not assigned, cf. discussion of the corresponding chloro complexes. It is likely that all the ligand field bands are obscured by charge transfer bands of high intensity. $^1$H and $^{13}$C NMR data are collected in Tables 5 and 6, respectively. The thiocyanato complexes exhibit similar pattern of resonances in their $^1$H NMR and $^{13}$C NMR spectra as described above for the corresponding chloro complexes. However, a single doublet appeared due to methyl protons on chiral carbon atoms in **5** instead of two doublets in its corresponding chloro complex, **1**. Moreover, an additional $^{13}$C NMR signal at 119–185 ppm appeared that is ascribed to the four thiocyanate–carbon nuclei. The above observations can be accounted for prevalence of same configuration and conformation in these complexes as their corresponding chloro complexes.

**Table 7.** Selected bond lengths (Å) and angles (deg) for **5**[a]

| | | | |
|---|---|---|---|
| Pd1–N1 | 2.0077(14) | Pd1–N4 | 2.0357(14) |
| N1–C2 | 1.492(2) | N1–C7$^i$ | 1.282(2) |
| N4–C3 | 1.487(2) | N4–C5 | 1.509(2) |
| Pd2–S11 | 2.3334(5) | Pd2–S21 | 2.3414(6) |
| S11–C11 | 1.6716(19) | S21–C21 | 1.6765(19) |
| C11–N11 | 1.155(3) | C21–N21 | 1.154(2) |
| N1–Pd1–N4 | 84.87(6) | N1–Pd1–N4$^i$ | 95.13(6) |
| Pd1–N1–C2 | 111.73(11) | Pd1–N1–C7$^i$ | 126.80(13) |
| Pd1–N4–C3 | 106.46(11) | Pd1–N4–C5 | 113.59(10) |
| S11–Pd2–S21 | 89.557(17) | S11–Pd2–S21$^{ii}$ | 90.443(17) |
| Pd2–S11–C11 | 108.54(6) | Pd2–S21–C21 | 105.90(6) |
| S11–C11–N11 | 175.55(18) | S21–C21–N21 | 179.76(1) |

[a] Symmetry operations *i*: $1\frac{1}{2} - x$, $\frac{1}{2} - y$, $1 - z$; and *ii*: $\frac{1}{2} - x$, $\frac{1}{2} - y$, $1 - z$.

### Crystal and molecular structure of 5

The molecular structures of the ionic components in **5** are shown in Fig. 2 and selected geometric parameters are collected in Table 7. In the cation, the palladium atom is coordinated by an $N_4$ donor set that defines a square-planar geometry; the palladium atom is located on a crystallographic centre of inversion. Confirmation of the formulation of the macrocyclic ligand, as shown in Fig. 1, is readily ascertained by an examination of the N–C bond distances, in particular the N1–C7$^i$ bond length of 1.282(2) Å, a distance reminiscent of a N=C double bond. The Pd–$N_{imine}$ bond distance of 2.0077(14) Å is significantly shorter than the Pd–$N_{amine}$ bond length of 2.0357(14) Å, in accord with expectation. In the anion, the palladium atom is also located at a centre of inversion and exists in a square-planar geometry, but this time defined by a $S_4$ donor set. Whereas deviations from the ideal 90° and 180° angles are minimal, the Pd–S bond distances at 2.3334(5) and 2.3414(6) Å are experimentally distinct, an observation that is related to intermolecular interactions, see below.

The $[Pd(SCN)_4]^{2-}$ anion has been observed crystallographically in 17 other non-disordered structures for which fractional atomic coordinates are available.[44] In each case, the palladium atom is located on a symmetry element. In fact, the 17 structures crystallize in three space groups only, i.e. $P-1$ (six examples), $P2_1/c$ or $P2_1/n$ (10) or $C2/c$ (1). It transpires that 16 structures feature the palladium atom on a centre of inversion and only one with palladium on a two-fold axis. The Pd–S bond distances within each complex anion are usually equal within experimental error but significant differences do exist in four examples. In the latter cases, the differences in Pd–S bonds are readily ascribed to the participation of one pair of thiocyanate ligands in intermolecular interactions. Overall, in the 17 literature structures, the Pd–S bond distances lie in the range 2.3138(9)–2.378(2) Å. In the present case, while the Pd–S bonds are experimentally distinct, they are quite close to each other and are midway between the above extremes.

The most notable feature of the crystal packing is the formation of charge-assisted N–H···N hydrogen bonding interactions

  

between the amine-H4 and the thiocyanate-N21 atoms; refer to Table 8 for a summary of the geometric parameters describing the most prominent intermolecular interactions.[45] These interactions lead to the formation of chains in the *c*-direction. These chains stack displaced by *c*/2 with respect to adjacent chains to form layers in the *bc*-plane so that each complex anion is surrounded by four complex cations as illustrated in Fig. 3. Stabilization to the layers is afforded by C–H···S interactions with the S11 atom participating in one such interaction and the S21 atom participating in three. The greater participation of the S21 atom in intermolecular interactions is deemed responsible for the elongation of the Pd–S21 bond with respect to the Pd–S11 bond, Table 7. Layers stack along the *a*-direction being held together weak C–H···N contacts, see Fig. 4.

### Anti-fungal activity

Studies on the antifungal activities of macrocycles and their complexes are restricted to some recent reports.[9–11,14–18] As an extension of this work, the investigation of the anti-fungal activities of $L^1$, $L_A$ $L_B$ and $L_C$ and their palladium(II) and palladium(IV) complexes against the five selectively phytopathogenic fungi

**Table 8.** Hydrogen bonding parameters (A–H···B; Å, deg) for **5**

| A | H | B | H···B | A···B | A–H···B | Symmetry operation |
|---|---|---|---|---|---|---|
| N4 | H4 | N21 | 2.17 | 3.061(2) | 161 | $1/2+x, 1/2-y, -1/2+z$ |
| C6 | H6b | S11 | 3.17 | 3.8525(19) | 128 | $1-x, y, 1/2-z$ |
| C2a | H2a2 | S21 | 3.23 | 4.144(2) | 156 | $1\,1/2-x, 1/2-y, 1-z$ |
| C5b | H5b2 | S21 | 3.22 | 4.134(2) | 156 | $1/2+x, 1/2+y, z$ |
| C6 | H6a | S21 | 3.26 | 4.2125(19) | 161 | $1/2+x, 1/2+y, z$ |
| C2 | H2 | N11 | 2.83 | 3.413(3) | 118 | $1/2+x, 1/2-y, 1/2+z$ |

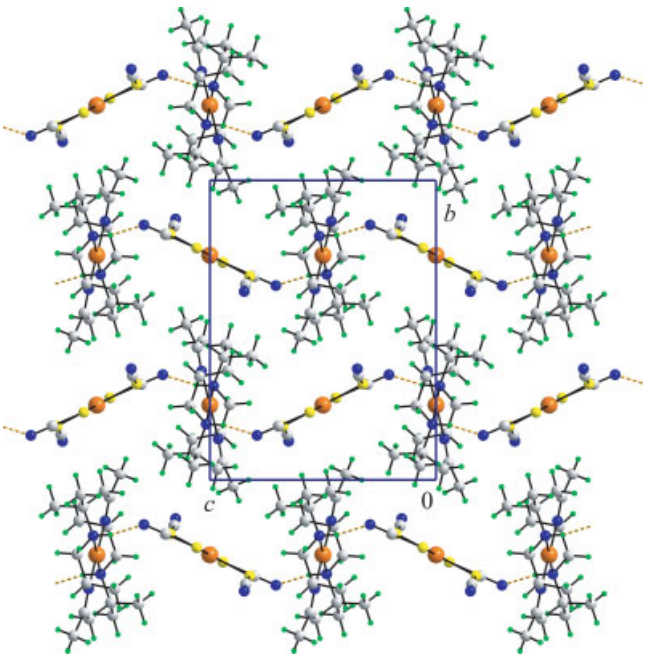


**Figure 3.** Supramolecular chains mediated by N–H···N interactions in the crystal structure of $[PdL^1][Pd(SCN)_4]$, **5**. Colour code: palladium, orange; sulfur, yellow; oxygen, red; nitrogen, blue; carbon, grey; hydrogen, green.

**Table 9.** Percentage inhibition of fungal radial mycelial growth by the ligands and their the test palladium complexes **1**–**8**[a]

| Ligands and complexes (100 µg d.w. $ml^{-1}$ PDA) | Percentage inhibition of mycelial growth | | | | |
|---|---|---|---|---|---|
| | *Macrophomina phaseolina* | *Curvularia lunata* | *Fusarium equiseti* | *Colletotrichums corcolei* | *Alternaria alternata* |
| $L^1 \cdot 2HClO_4$ | 33 | 16 | n.d. | n.d. | 22 |
| **1** | 38 | 38 | 75 | 63 | 38 |
| **5** | 38 | 38 | 75 | 63 | 38 |
| $L_A$ | 30 | 22 | 25 | 25 | 28 |
| **2** | 38 | 38 | 17 | 63 | 38 |
| **6** | 38 | 38 | 58 | 63 | 38 |
| $L_B$ | 30 | 10 | 21 | 21 | 26 |
| **3** | 38 | 38 | 75 | 62 | 38 |
| **7** | 38 | 38 | 75 | 63 | 38 |
| $L_C$ | 31 | 13 | 21 | 19 | 26 |
| **4** | 38 | 38 | 75 | 63 | 38 |
| **8** | 38 | 38 | 75 | 63 | 38 |
| Nystatin | 76 | 70 | 45 | 41 | 51 |

[a] d.w. = dry weight; n.d. = not determined.

**Table 10.** Anti-bacterial screening of the ligands and their palladium complexes **1**–**8** against some Gram-positive bacteria[a]

| Ligands and complexes (200 µg d.w./disc) | Zone of inhibition in mm after 24 and 48 h | | | | | | | |
|---|---|---|---|---|---|---|---|---|
| | *B. cereus* | | *B. subtilis* | | *S. aureus* | | *B. magaterium* | |
| | 24 h | 48 h | 24 h | 48 h | 24 h | 48 h | 24 h | 48 h |
| $L^1$ | 0 | n.d. | 0 | n.d. | 0 | n.d. | 0 | n.d. |
| **1** | 15 | 18 | 15 | 15 | 15 | 15 | 15 | 15 |
| **5** | 5 | 8 | 8 | 8 | 0 | 0 | 10 | 10 |
| $L_A$ | 17 | n.d. | n.d. | n.d. | n.d. | n.d. | n.d. | n.d. |
| **2** | 10 | 14 | 12 | 12 | 0 | 0 | 10 | 10 |
| **6** | 0 | 0 | 0 | 0 | 0 | 0 | 0 | 0 |
| $L_B$ | 15 | n.d. | 6 | n.d. | 5.5 | n.d. | 0 | n.d. |
| **3** | 15 | 15 | 15 | 15 | 0 | 0 | 10 | 10 |
| **7** | 0 | 0 | 0 | 0 | 0 | 0 | 0 | 0 |
| $L_C$ | 19 | n.d. | n.d. | n.d. | n.d. | n.d. | n.d. | n.d. |
| **4** | 0 | 10 | 10 | 10 | 0 | 0 | 5 | 5 |
| **8** | 8 | 8 | 8 | 8 | 0 | 0 | 0 | 0 |
| Ampicillin (20 µg d.w./disc) | 16 | n.d. | 25 | n.d. | 24 | n.d. | 19 | n.d. |

[a] d.w. = dry weight; 0 = no inhibition; n.d. = not determined.

*Macrophomina phaseolina, Curvularia lunata, Fusarium equiseti, Colletotrichum corcolei* and *Alternaria Alternata* has been undertaken. These are phytopathogens of important crop plants such as jute, chilli and aubergine, and can cause significant economic loss to the farming community. The control of the pathogens by non-hazardous fungicides is the desired outcome of this type of research, especially as fungi species are gradually becoming resistant to fungicides. The anti-fungal activity data of these compounds, as well as that of nystatin for comparison, are collated in Table 9. It is evident that the macrocycles and their complexes show some anti-fungal activity. Generally, previous studies have shown that the activity of the macrocyclic ligands decreases

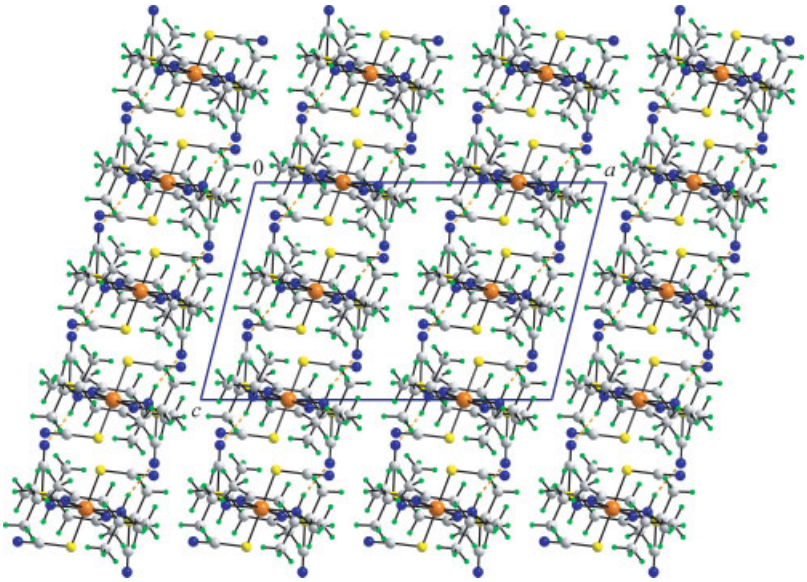


**Figure 4.** View of the crystal packing of $[PdL^1][Pd(SCN)_4]$, **5**, viewed in projection down the *b*-axis. Hydrogen-bonding interactions are shown by orange dashed lines. Colour code: palladium, orange; sulfur, yellow; oxygen, red; nitrogen, blue; carbon, grey; hydrogen, green.

**Table 11.** Anti-bacterial screening of the ligands and their test palladium complexes **1**–**8** against some Gram-negative bacteria[a]

| Ligands and complexes (200 µg d.w./disc) | Zone of inhibition in mm after 24 and 48 h | | | | | | | | | | | |
|---|---|---|---|---|---|---|---|---|---|---|---|---|
| | *E. coli* | | *V. cholerae* | | *S. typhe* | | *S. paratyphi* | | *Pse. species* | | *S. dysenterie* | |
| | 24 h | 48 h | 24 h | 48 h | 24 h | 48 h | 24 h | 48 h | 24 h | 48 h | 24 h | 48 h |
| $L^1 \cdot 2HClO_4$ | 0 | n.d. | 0 | n.d. | 7 | n.d. | 0 | n.d. | 0 | n.d. | 5.5 | n.d. |
| **1** | 15 | 16 | 15 | 15 | 10 | 15 | 12 | 12 | 15 | 15 | 8 | 12 |
| **5** | 8 | 8 | 0 | 0 | 0 | 8 | 8 | 8 | 0 | 0 | 0 | 5 |
| $L_A$ | 6 | n.d. | n.d. | n.d. | 12 | n.d. | n.d. | n.d. | n.d. | n.d. | 12 | n.d. |
| **2** | 10 | 15 | 6 | 6 | 10 | 18 | 15 | 15 | 0 | 0 | 10 | 13 |
| **6** | 0 | 0 | 0 | 0 | 0 | 0 | 0 | 0 | 0 | 0 | 0 | 0 |
| $L_B$ | 21 | n.d. | 6 | n.d. | 8 | n.d. | 0 | n.d. | 0 | n.d. | 10 | n.d. |
| **3** | 8 | 10 | 8 | 8 | 8 | 10 | 15 | 15 | 0 | 0 | 8 | 8 |
| **7** | 0 | 0 | 0 | 0 | 0 | 0 | 0 | 0 | 0 | 0 | 0 | 0 |
| $L_C$ | 7 | n.d. | n.d. | n.d. | 10 | n.d. | n.d. | n.d. | n.d. | n.d. | 8 | n.d. |
| **4** | 0 | 0 | 0 | 0 | 10 | 12 | 10 | 10 | 0 | 0 | 0 | 8 |
| **8** | 0 | 0 | 0 | 0 | 0 | 0 | 0 | 8 | 0 | 0 | 0 | 0 |
| Ampicillin (20 µg d.w./disc) | 30 | n.d. | 32 | n.d. | 25 | n.d. | 28 | n.d. | 35 | n.d. | 35 | n.d. |

[a] d.w. = dry weight; 0 = no inhibition; n.d. = not determined.

upon coordination,[9–11,14–18] but in the present study the palladium complexes behave differently. Thus, most of the complexes exhibit greater anti-fungal activities than their corresponding ligands as well than that exhibited by the corresponding copper(II), nickel(II), cobalt(III), zinc(II) and cadmium(II) complexes (S. K. Hazari, T. G. Roy and A. Dutta, unpublished results).[9–11,14–18] In earlier studies it was observed that the extent of inhibition depends on the particular type of macrocyclic ligand and on the axial ligand/counterion (e.g. chloride, bromide, iodide, perchlorate and thiocyanate), but in the present case, it is noted that the extent of inhibition is independent of the nature of macrocyclic ligand as well as of the axial ligand/counterion (chloride and thiocyanate).

In case of *Fusarium equiseti*, the inhibition (75%) of all complexes except **2** was found to show much higher activities than the standard antibiotic Nystatin (45%). All complexes were found to be more effective inhibitors towards *Colletrotrichum corcolei* (63%) compared with the standard Nystatin.

From the above discussion it can be concluded that the nature of ligands and metals plays a significant role in the inhibition of mycelial growth. However, in order to understand the functions responsible for anti-fungal activities of these macrocycles and their complexes, more studies are necessary.

## Anti-bacterial activity

Except a very few recent reports,[10,16,18] the anti-bacterial activity of macrocycles and their complexes has so far not been studied to any great extent. Herein, investigations on the anti-bacterial

  

activity of the ligands and their palladium complexes as well as that of commercially important anti-bacterial agent ampicillin have been carried out. The selected Gram-positive and Gram-negative bacteria can cause fatal diseases, viz. *Salmonella typhi* causes typhoid, *Shigella dysenteriae* causes dysentery, and *Escherichia coli* and *Bacillus cerelus* cause gastroenteritis. The results, summarized in Tables 10 and 11, show that, while the ligands are ineffective in some cases, several of their complexes exhibit some anti-bacterial activity. This is in accord with observations on similar systems.[10,16,18] Only $L_A$ and $L_C$ exhibit greater activities against *E. coli*. It is particularly interesting to note that the chloro complexes exhibit, in almost all cases, greater activity than the corresponding thiocyanato complexes.

As seen from Tables 10 and 11, complexes **1**–**5** were effective against both Gram-positive and Gram-negative bacteria. Complex **8** was effective only against some Gram-positive bacteria. By contrast, neither **6** nor **7** showed observable activity against either Gram-positive or Gram-negative bacteria. No definitive trends can be derived from the observations at this stage but the positive results suggest further studies are warranted.

### Acknowledgements

The authors thank the University Grants Commission of Bangladesh for a fellowship to K.K.B. and the Ministry of Science, Information and Communication Technology, Government of People's Republic of Bangladesh, for a grant and a fellowship to T.G.R. The grant of a stipend to T.G.R. by the Korea Science and Engineering Fellowship (KOSEF) is gratefully acknowledged. The authors thank Professor N. Anwar, Department of Microbiology, University of Chittagong, for his support of the anti-fungal and anti-bacterial studies.

### Supporting information

Supporting information may be found in the online version of this article.

## References

[1] P. V. Benhardt, G. A. Lawrance, *Coord. Chem. Rev.* **1990**, *104*, 197.
[2] G. Reid, M. Schroder, *Chem. Soc. Rev.* **1990**, *19*, 239.
[3] T. J. Norman, D. Parker, F. C. Smith, D. J. King, *J. Chem. Soc. Chem. Commun.* **1995**, 1879.
[4] B. Konig, M. Pelka, H. Zieg, P. G. Jones, I. Dix, *Chem. Commun.* **1996**, 471.
[5] A. C. Hollinshead, P. K. Smith, *Antibiotics Ann.* **1990**, *313*, 1959; *Chem. Abstr.* **1960**, *54*, 761.
[6] S. D. Samant, R. A. Kulkarni, *J. Ind. Chem. Soc.* **1979**, *56*, 1002.
[7] M. P. Suh, H. R. Moon, E. Y. Lee, S. Y. Jang, *J. Am. Chem. Soc.* **2006**, *128*, 4710.
[8] A. K. Singh, A. Kumar, S. Panwar, S. Baniwal, *Analyst* **1999**, *124*, 521.
[9] T. G. Roy, S. K. S. Hazari, B. K. Dey, H. A. Meah, M. S. Rahman, D. I. Kim, Y. C. Park, *J. Coord. Chem.* **2007**, *40*, 1567.
[10] T. G. Roy, S. K. S. Hazari, B. K. Dey, H. A. Miah, F. Olbrich, D. Rehder, *Inorg. Chem.* **2007**, *46*, 5372.
[11] T. G. Roy, S. K. S. Hazari, B. K. Dey, A. Nath, N. Anwar, D. I. Kim, E. H. Kim, Y. C. Park, *J. Incl. Phen. Mac. Chem.* **2007**, *58*, 249.
[12] T. Yamuchi, S. Nakajima, M. Hirayama, K. Kojiri, H. Suda, Banyu Pharmaceutical Co., Japan, **1998**.
[13] H. Arai, Y. Matshima, T. Eguchi, S. Kazutoshi, K. Katsumi, *Tetrahedron Lett.* **1998**, *39*, 3181.
[14] S. K. S. Hazari, T. G. Roy, B. K. Dey, S. C. Das, E. R. T. Tiekink, *Metal-Based Drugs* **1997**, *4*, 255.
[15] T. G. Roy, S. K. S. Hazari, B. K. Dey, S. Chakraborty, E. R. T. Tiekink, *Metal-Based Drugs* **1999**, *6*, 345.
[16] T. G. Roy, S. K. S. Hazari, B. K. Dey, H. A. Miah, C. Bader, D. Rehder, *Eur. J. Inorg. Chem.* **2004**, 4115.
[17] T. G. Roy, S. K. S. Hazari, B. K. Dey, R. Sutradhar, L. Dey, N. Anowar, E. R. T. Tiekink, *J. Coord. Chem.* **2006**, *59*, 351.
[18] T. G. Roy, S. K. S. Hazari, B. K. Dey, S. Dutta, M. A. Monchur, E. R. T. Tiekink, *J. Coord. Chem.* **2006**, *59*, 1757.
[19] T. G. Roy, S. K. S. Hazari, B. K. Dey, H. A. Miah, E. R. T. Tiekink, *Acta Crystallogr.* **2001**, *E57*, 524.
[20] T. G. Roy, R. Bembi, S. K. S. Hazari, B. K. Dey, T. K. Acharjee, E. Horn, E. R. T. Tiekink, *J. Coord. Chem.* **2002**, *55*, 853.
[21] R. E. Benson, T. G. Roy, S. K. S. Hazari, K. K. Barua, E. R. T. Tiekink, *Acta Crystallogr.* **2006**, *E62*, 1968.
[22] S. K. S. Hazari, T. G. Roy, K. K. Barua, E. R. T. Tiekink, *J. Chem. Cryst.* **2008**, *38*, 1.
[23] N. F. Curtis, D. A. Swann, T. N. Waters, I. E. Maxwell, *J. Am. Chem. Soc.* **1969**, *91*, 4588.
[24] T. G. Roy, R. Bembi, *Bangl. Chem. Soc.* **2002**, *15*, 23; *Chem. Abstr.* **2003**, *139*, 230266.
[25] R. Bembi, S. M. Sondhi, A. K. Singh, R. Singh, T. G. Roy, A. K. Jhanji, J. W. Lown, R. G. Ball, *Bull. Chem. Soc Jpn.* **1989**, *62*, 3701.
[26] T. Higashi, ABSCOR. Rigaku Corporation, Tokyo, **1995**.
[27] CrystalClear. *User Manual*. Rigaku/MSC Inc., The Woodlands, TX, **2005**.
[28] P. T. Beurskens, G. Admiraal, G. Beurskens W. P. Bosman, S. García-Granda, J. M. M. Smits, C. Smykalla, The DIRDIF program system, Technical Report of the Crystallography, Laboratory, University of Nijmegen, Nijmegen, **1992**.
[29] G. M. Sheldrick, *Acta Crystallogr.* **2008**, *A64*, 211.
[30] C. K. Johnson, ORTEP II, Report ORNL-5136. Oak Ridge National Laboratory, Oak Ridge, **1976**.
[31] *Crystal Impact, DIAMOND*. Version 3.1c. Crystal Impact GbR, Bonn, **2006**.
[32] *teXsan, Structure Analysis Package*. Molecular Structure Corporation: Houston, TX, **1992**.
[33] A. L. Spek, *J. Appl. Crystallogr.* **2003**, *36*, 7.
[34] M. Hashimoto, K. Sakata, *Polyhedron* **1966**, *16*, 975.
[35] D. I. Kim, E. H. Kim, J. C. Byun, J. H. Choi, H. G. Na, Y. C. Park, *J. Cord. Chem.* **2000**, *55*, 505.
[36] B. Bosnik, C. K. Poon, M. L. Tobe, *Inorg. Chem.* **1965**, *4*, 1102.
[37] R. Bembi, M. G. B. Drew, R. Singh, T. G. Roy, *Inorg. Chem* **1991**, *30*, 1403.
[38] R. W. Hay, D. A. House, R. Bembi, *J. Chem. Soc. Dalton Trans.* **1984**, 1927.
[39] T. W. Hambley, *J. Chem. Soc. Dalton Trans.* **1986**, 565.
[40] R. Bembi, S. M. Sondhi, A. K. Singh, A. K. Jhanji, T. G. Roy, J. W. Lown, R. G. Ball, *Bull. Chem. Soc. Jpn.* **1989**, *62*, 3701.
[41] M. Nakamoto, *Infrared Spectra of Inorganic and Coordination Compounds*. Wiley: New York, **1963**.
[42] F. H. Allen, *Acta Crystallogr.* **2002**, *B58*, 380.
[43] T. Steiner, G. R. Desiraju, *Chem. Commun.* **1997**, 891; b) G. R. Desiraju, T. Steiner, *The Weak Hydrogen Bond in Structural Chemistry and Biology*. Oxford University Press/International Union of Crystallography, **2001**; c) R. A. Howie, G. M. de Lima, D. C. Menezes, J. L. Wardell, S. M. S. V. Wardell, D. J. Young, E. R. T. Tiekink, *CrystEngComm* in press.

  